



## Comparison of Frequency Selective Surface (FSS) Filter Performance Between Square and Hexagon Shape for GPS Jamming Application

Nur Afiqah Alfian<sup>1</sup>, Nurhakimah Norhashim<sup>1,\*</sup>, Nadhiya Liyana Mohd Kamal<sup>1</sup>, Zulhilmy Sahwee<sup>1</sup>, Shahrul Ahmad Shah<sup>1</sup>, Mohd Amzar Azizan<sup>2</sup>

<sup>1</sup> Unmanned Aerial System Research Laboratory, Avionics Section, Malaysia Institute of Aviation Technology, Universiti Kuala Lumpur, 43800, Dengkil, Malaysia

<sup>2</sup> The Higher Technology College – Khalifa bin Zayed Air College Abu Dhabi, UAE

### ABSTRACT

Intentionally disrupting electromagnetic signals, known as jamming, is a major risk to communication and navigation systems, especially in the case of Unmanned Aerial Vehicles (UAVs). This study examines the effectiveness of Frequency Selective Surface (FSS) filters in reducing jamming interference by comparing square and hexagon shaped FSS arrangements. The effectiveness of FSS filters require to achieve by reducing a 1.6 GHz jamming signal while maintaining continuous communication signals at 2.4 GHz between UAVs and remote stations. Both square and hexagonal shapes is compared where components are oriented at 90-degree angles in both rows and columns, diverging from the conventional 45-degree adjacency pattern. FSS structures is analysed at 2.4 GHz using Ansys HFSS software to attenuation at 1.6 GHz. The main results show that the square loop FSS has better attenuation performance, reaching -0.4 dB at 1.6 GHz and -49.0 dB (simulated) at 2.4 GHz, compared to the hexagon loop FSS. This study highlights the capability of FSS filters to effectively combat jamming threats in GPS systems, with potential benefits for improving communication security in national defence and civilian industries.

#### Keywords:

Jamming; Unmanned Aerial Vehicle (UAV); square shape; hexagon shape; Frequency Selective Surface Filter (FSS); filter performance; reflection coefficient

### 1. Introduction

The expansion of wireless technology has sparked significant interest in its security implications. Electromagnetic interference is defined as an unregulated electromagnetic wave can lead to the malfunction of electrical devices in vulnerable settings as conducted by Jin *et al.*, [1]. Many researchers have studied the Frequency Selective Surface (FSS) filter because of its extensive use in filtering certain frequency [2]. Jamming is the deliberate use of electromagnetic energy to interfere with signal transmission and reception in a communication or navigation system [3,4] by sending a powerful signal to disrupt the communication of Unmanned Aerial Vehicles (UAVs) and force them to land [5,6]. This prevents the operator from accessing data from the UAVs, resulting in a loss of control over the UAV. Jamming actions present a substantial risk to the communication security of

\* Corresponding author.

E-mail address: nurhakimah@unikl.edu.my

<https://doi.org/10.37934/araset.XX.X.132142>

the country, affecting both national and civilian sectors. An FSS filter is an alternative method used to minimize interference [7]. FSS filters are engineered surfaces that selectively manage the transmission as proclaimed by Jang *et al.*, [8] or reflection as enunciated by Pieper *et al.*, [9] of electromagnetic waves according to their frequency.

The FSS filter can be classified into various types of filters, including low pass, high pass, band stop, and band pass, as illustrated in Figure 1. A low pass FSS filter permits frequencies below a specific cutoff frequency and suppresses higher frequencies as affirmed by Fallahi *et al.*, [10]. A high pass filter allows frequencies above a specific cutoff frequency while reducing the amplitudes of lower frequencies as mentioned by Amin *et al.*, [11]. It permits signals over a set threshold frequency while inhibiting lower frequencies. A band stop filter known as a notch filter, suppresses signals within a particular frequency range but permits frequencies outside of this range [12]. As conducted by Kapoor *et al.*, [13] a band pass filter is a permits signals within a specific frequency range with minimal attenuation, while reducing the strength of frequencies outside this range.

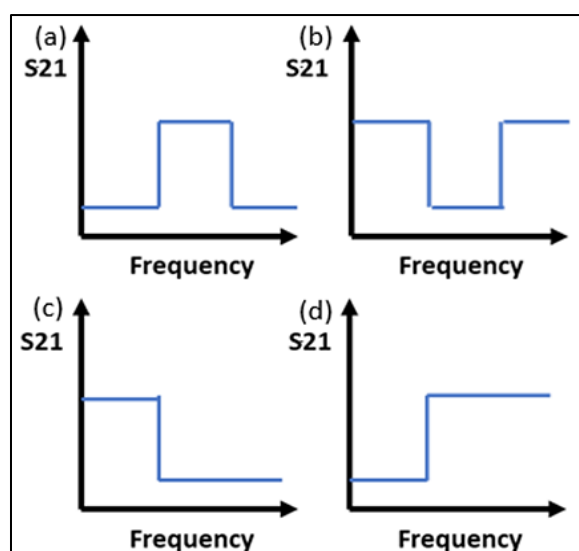


**Fig. 1.** The illustration of types of filters (a) Band pass filter (b) Band stop filter (c) Low pass filter (d) High pass filter

The bandpass has been designed to meet the criteria for  $S_{11}$  and  $S_{21}$  parameters to attenuate signals at 1.6 GHz while permitting only signals at 2.4 GHz to pass through. The bandpass filter is chosen for designing the FSS and provides several building methods and components including resonant circuits, waveguides, or transmission lines as conducted by Al-Joumayly and Behdad [14]. An aperture element FSS act as a high-pass filter as asserted by Debarros *et al.*, [15] means that it exhibits low-frequency reflection and high-frequency transmission. On the other hand, a patch-element FSS, resembling a low-pass filter, predominantly permits lower frequencies to transmit while reflecting higher frequencies as conducted by Campos *et al.*, [16] and Anwar *et al.*, [17]. Several factors in FSS design influence the frequency response, including substrate thickness, substrate dielectric, geometry, element spacing, slot size, and others as mentioned by Luo *et al.*, [18] and Hussin *et al.*, [19].

FSS filters design have evolved from a fundamental configuration to encompass designs characterized by circles, Jerusalem crosses, and hexagons. These configurations are categorized according to their respective functionalities and the elicited responses such Group-1 (centrally connected or N-poles), Group-2 (looped shapes), Group-3 (solid interiors or patch shapes), and

Group-4 (combinations of the Group 1 and Group-2) [16]. Bandpass FSS filters are available in several forms including square and hexagon. The square FSS design is known for its simplicity, ease of production [20] and cost-effectiveness and reproducibility as mentioned by Ghezzi *et al.*, [21]. Square FSS structures might experience elevated sidelobe levels, which can potentially degrade filter effectiveness, especially in suppressing unwanted frequency components. Hexagonal FSS arrangements offer distinct advantages by reducing sidelobes and improving filter selectivity [22-24]. Hexagonal structures' intrinsic symmetry enhances spectral performance by minimising spurious responses and improving the filter's ability to isolate certain frequency bands as conducted by H. Bin Wang and Cheng [25]. However, fabricate hexagonal FSS filters may be more sophisticated than square ones, which could lead to higher manufacturing intricacies and expenses.

This paper investigates the efficacy of square loop and hexagon loop bandpass FSS at frequencies of 1.6 GHz and 2.4 GHz. This paper will examine the comparative characteristics of square and hexagonal shapes, where components are oriented at 90-degree angles in both rows and columns, diverging from the conventional 45-degree adjacency pattern. Numerous factors contribute to the final configuration when utilizing a 90-degree orientation as mentioned by [22,26,27]. Section 1 provides contextual background for FSS filter design solutions to address drawbacks in UAV systems. The second chapter offers methodology encompasses a detailed exposition of Ansys simulation for square and hexagon shaped FSS configurations. In third section, results and analysis presents a thorough examination of the comparative efficacy of square and hexagon shaped FSS arrangements. At last section provide potential shape bandpass FSS filters to enhance communication security within UAV systems are explored.

## 2. Methodology

### 2.1 Simulation Using ANSYS Software

The performance of the square and hexagon band pass FSS filters was modelled using the ANSYS HFSS simulation to design and simulate the return loss ( $S_{11}$ ) and insertion loss ( $S_{21}$ ). Floquet-mode ports were utilised, assuming an infinite array of square and hexagonal unit cell loops. The bandpass filter is designed for approximately 5 cm x 5 cm in size. A comparative analysis was conducted on the performance of bandpass FSS utilizing identical ideal dielectric substrates [17]. Square shape bandpass filter, depicted in Figure 2(a), is selected for their resonance at lower frequencies, ease of production, optimal use of space, and ability to accommodate longer wavelengths whilst hexagon-shaped filters Figure 2(b), are being studied for their natural symmetry resulting in consistent behaviour throughout the structure and uniform filtering characteristics.

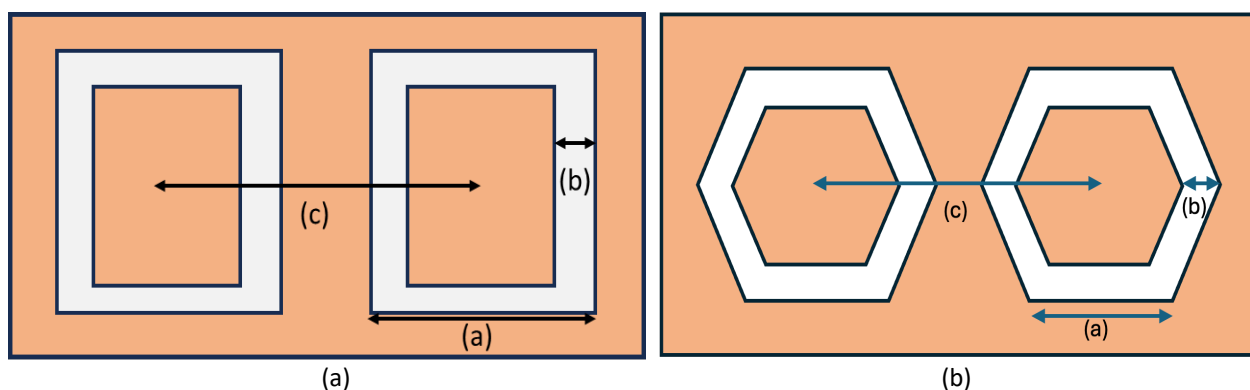


Fig. 2. (a) Square bandpass filter and its parameters (b) Hexagon bandpass filter and its parameters

Optimising symmetry enhances the coverage of the FSS by reducing wasted space, which is essential for efficient use in large-scale applications or strict size limitations. Hexagonal structures may sustain several resonant modes, allowing for complex filtering abilities. Arranging hexagonal elements in precise configurations reduces interference and crosstalk among adjacent elements, improving the overall filter's effectiveness including factors of periodic size ( $p$ ), length of edge of each element ( $l$ ), and aperture width ( $w$ ) are crucial aspects to consider during the design phase, as outlined in Table 1.

Square and hexagon filters have insulating substrates with openings mainly dielectric, that maintains a stable material value. The square filter uses copper for its conductor patch and plastic for the aperture, and the same material for hexagon filter. Number of arrays for both shapes are typically specified in dimensions such as  $2 \times 2$ ,  $2 \times 3$ , or  $4 \times 4$  to guarantee the optimum filter performance. The filters' dimensions are 240 mm as shown in Figure 3 due to the practicality of experimental testing in an anechoic room considering the compatibility with the size of transmitting and receiving antennas. The filter arrays' dimensions, represented as an  $a$  and  $b$ , where both are equal in value as number of arrays selected in this study is  $4 \times 4$  due to its dimension fit to cover bottom of GPS module size should be proportional to the antennas utilized for signal transmission and reception.

**Table 1**  
 Parameters depicted in each shape designation

Parameter	Indicator	Description
$a$	$l$	Length of edge (array size)
$b$	$w$	Aperture width
$c$	$p$	Periodic length

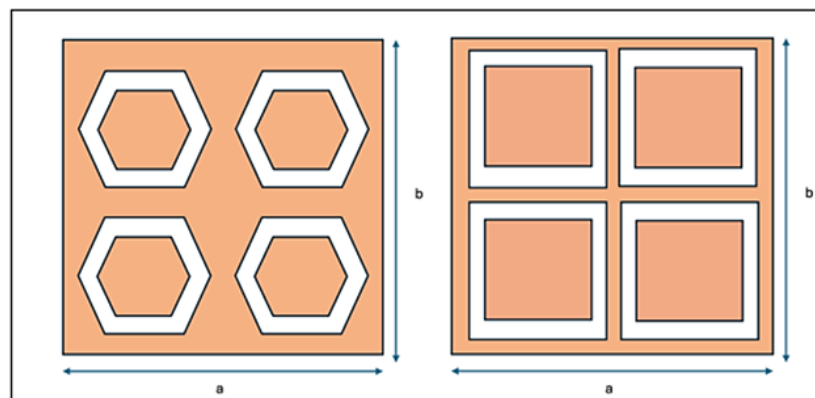


**Fig. 3.** Size of array =  $2 \times 2$ , where  $a=b=240\text{mm}$

## 2.2 Impact of Parameters on Bandpass FSS filter

Changing the periodic size ( $p$ ), length of edge of each element ( $l$ ), and aperture width ( $w$ ) significantly influences the performance of square and hexagon-shaped FSS filters. In FSS resonance, the circumference of the elements must be aligned with the wavelength, which is determined by the effective permittivity and inter-element spacing. Narrowing the gap between shapes usually results in a wider bandwidth. Yet, this decrease also elevates inter-element capacitance, causing the resonant frequency to shift towards the lower range. To counteract this affect and uphold the intended resonance frequency, modifications to the elements' radius may be required. The size of the array, determined by adjusting the periodic length ( $p$ ), has a substantial impact on the filter's

resonance frequency and overall performance. This will affect multiple parameter such as frequency response, bandwidth, transmission, and reflection qualities. It is crucial to thoroughly evaluate these aspects when modifying the periodic length to achieve the optimum filter performance for square and hexagon shaped FSS setups.

### 3. Results

#### 3.1 Simulation of Length of Edge on Each Element

The design simulations for square shape involve varying the period ( $p$ ) from 10 mm to 50 mm in increments of 10mm, a constant aperture width ( $w$ ) = 2 mm. The ideal length of 30 mm is established according to the simulated  $S_{11}$  and  $S_{21}$  values. Square and hexagonal FSS filters operate using transmission and reflection coefficients, known as  $S_{11}$  and  $S_{21}$ .  $S_{11}$  describes how incident electromagnetic waves are reflected by the FSS structure, indicating the filter's capability to block specific frequencies.  $S_{21}$  quantifies the transmission of electromagnetic waves through the FSS, showing the filter's passband properties. The hexagon-shaped filter with the radius length also known as length of edge of each element ( $l$ ), varies incrementally from 10 mm to 20 mm in intervals of 10 mm. The simulations are fixed on period ( $p$ ) of 50 mm and aperture width ( $w$ ) of 2 mm. The ideal radius length is achieved at 20 mm. Figure 4 shows resonant frequencies corresponding to transient zeroes for circumference values at 20 mm, suggesting effective transmission at these frequencies. The perimeter of the hexagon can be calculated by multiplying the length of one side by 6. This calculation is based on placeholder values of a 20 mm side length and aperture width ( $w$ ) of 2 mm.

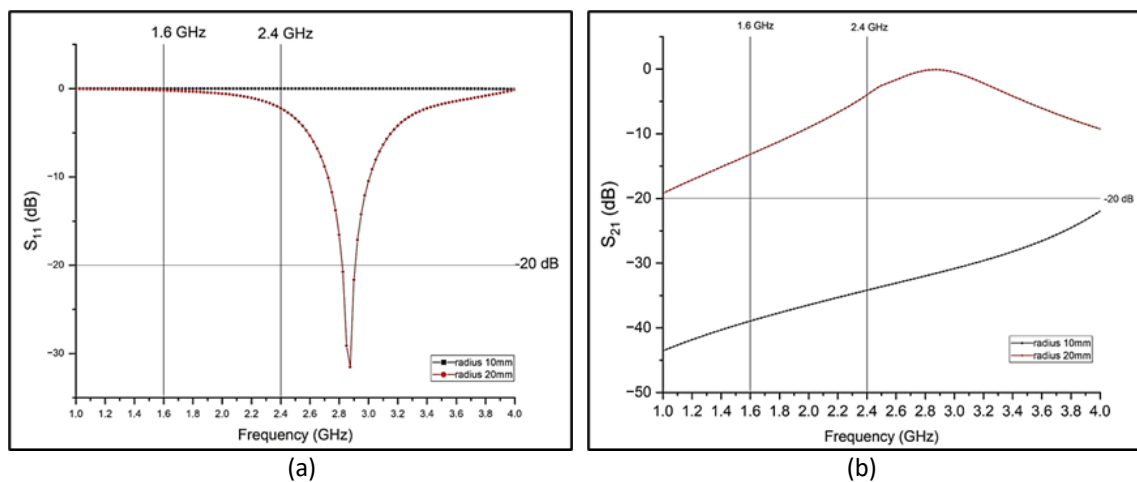


**Fig. 4.** (a) Reflection coefficient  $S_{11}$  of hexagon ( $p = 50$  mm,  $w = 2$  mm) with varying lengths (b) Transmission coefficient  $S_{21}$  of hexagon ( $p = 50$  mm,  $w = 2$  mm) with varying lengths

Figure 5 below shows a comparison of square and hexagon bandpass filters on (a) reflection coefficient and (b) transmission coefficient when adjusting the length of edge of each element. The square and hexagon-shaped filters demonstrate stability and nearly optimum performance with certain parameter settings. For the square design, when the outputs stabilise and approach optimal values between 30 mm and 40 mm, the measurement interval then is decreased from 10 mm to 2 mm within this range. Stability and near-optimal performance are attained with a radius length of 20 mm for the hexagon-shaped filter. The measuring interval has been decreased from 10 mm to 2 mm for each measurement taken within the range of 20 mm to 30 mm. When the radius is larger than 26 mm the element shapes clash with neighbouring cells, as shown in the red box in the Figure 6.

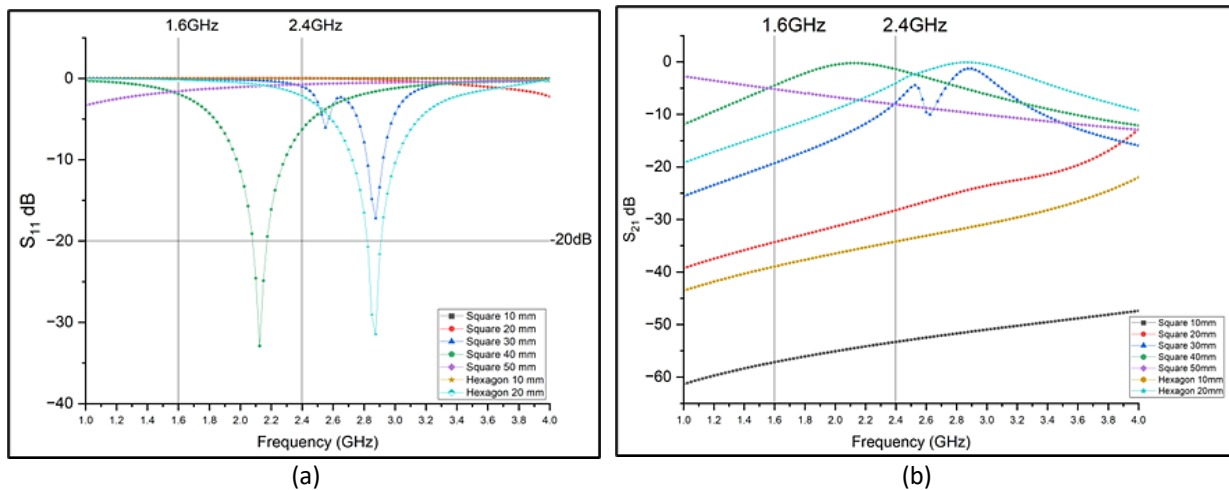


**Fig. 5.** (a) Comparisons of reflection coefficient  $S_{11}$  between square and hexagon with varying lengths (interval: 10 mm) (b) Comparisons of transmission coefficient  $S_{21}$  between square and hexagon with varying lengths (interval: 10 mm)

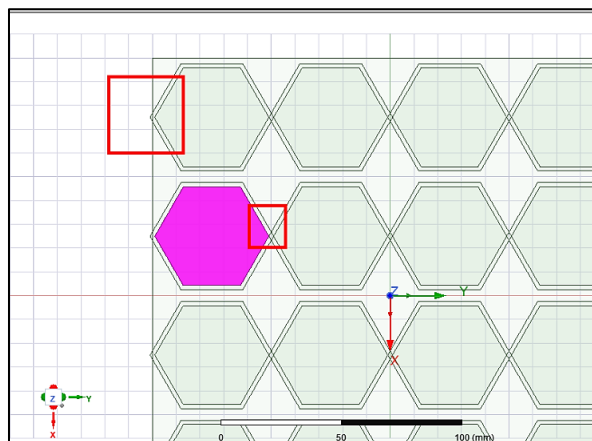


**Fig. 6.** Investigation of hexagonal cell interactions within a cellular array

The square filter with length of 38 mm improving to reduce 1.6 GHz interference signals while enabling smooth transmission around 2.4 GHz as shown in Figure 7. For the transient pole to shift to right, 2.4 GHz, adjustments in the aperture width size are required to accurately resonate  $S_{11}$  and  $S_{21}$  values at 2.4 GHz. The square's size should be roughly proportional to the wavelength of the chosen frequency range, with larger squares maybe needed for lower frequencies. The hexagon-shaped filter, depicted in Figure 7(b), delivers the desired effect with length 24 mm. The hexagon's size should match the wavelength of the chosen frequency range, maybe necessitating larger hexagons for lower frequencies. Square shape with length of 38 mm for each element, and hexagon with length of 24 mm are then selected on other parameters such as aperture width ( $w$ ) and periodic size ( $p$ ) as shown in Figure 8.

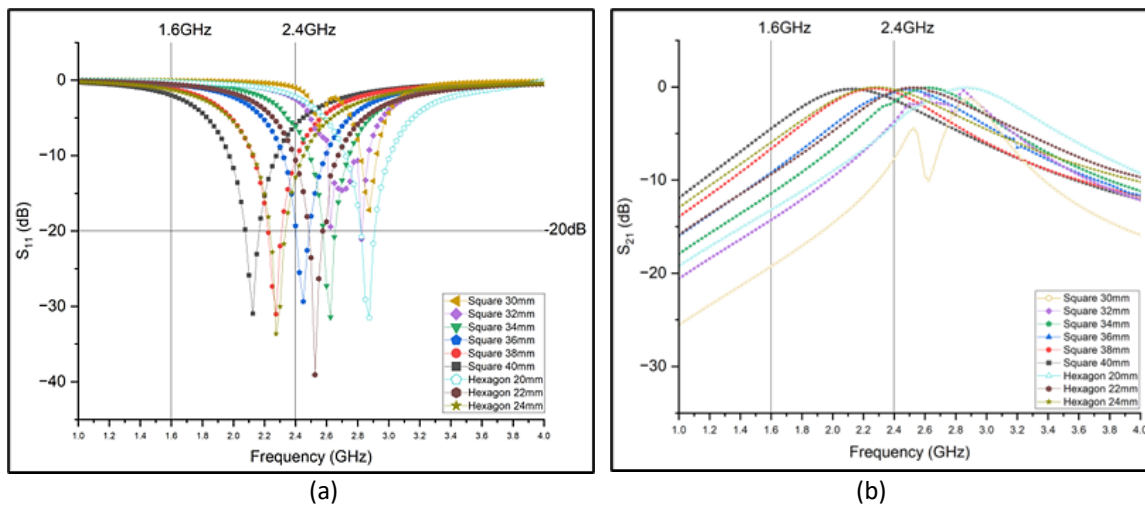


**Fig. 7.** (a) Comparison of reflection coefficient  $S_{11}$  between square (30-40 mm) and hexagon (20-24 mm) with varying lengths (interval: 2 mm) (b) Comparison of transmission coefficient  $S_{21}$  between square (30-40 mm) and hexagon (20-24 mm) with varying lengths (Interval: 2 mm)

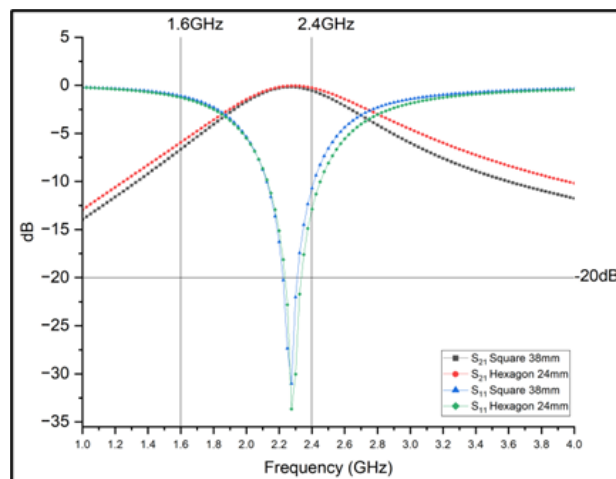


**Fig. 8.** Comparison of square = 38 mm and hexagon = 24 mm at fixed Lengths

### 3.2 Effect of Width Aperture ( $w$ ) on the Filter Performance

The aperture width ( $w$ ) is varied from 1 mm to 10 mm with a 0.1 mm increment. The analysis shows that widths of 2.5 mm and 3.0 mm have  $S_{21}$  values closest to 0 at 2.4 GHz, and  $S_{11}$  approaches 1 at 1.6 GHz. The hexagon shape has a fixed radius of 24 mm and a period of 50 mm, selected to potentially provide the best results while yet permitting modifications in other factors such as aperture width and period size. The  $w$  ranges are varied similar with square shape. The transmission frequency with the lowest  $S_{11}$  value at 2.4 GHz corresponds to an aperture width between 2.8 to 3.0 mm, consistent with the results for  $S_{21}$ . This indicates that there is uniformity in performance for both parameters to ensure the filter operates at its optimum. Both square and hexagon-shaped filters show comparable behaviour when the aperture width ( $w$ ) increases. When increasing the aperture width ( $w$ ) for both square and hexagon, the transient poles at the  $S_{11}$  port to shift to the right, leading to a fall in the  $S_{11}$  value at 2.4 GHz from infinity to 0. As a result, there is a decrease in the transmission of 2.4 GHz through the filter. As the aperture width ( $w$ ) lowers, the transient poles of both geometries align with the resonance frequency of 2.4 GHz. Transient poles align with the resonance frequency



of 2.4 GHz within the aperture width range of 2.0 mm to 3.0 mm for the hexagon shape, as shown in the Figure 9.

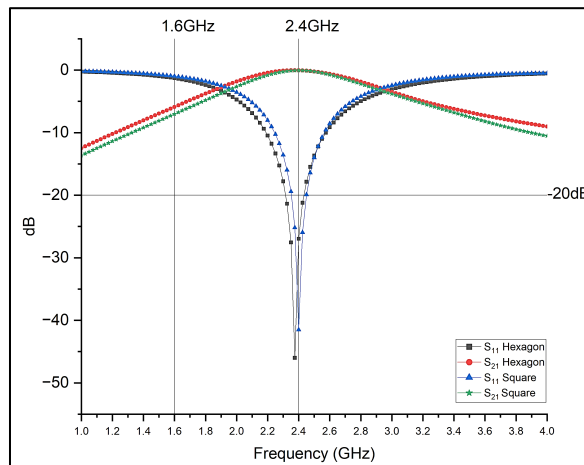


**Fig. 9.** Comparison of square and hexagon shapes with a period=50 mm and width = 2.9 mm

The hexagon shape requires more simulations with narrower intervals for the aperture width ( $w$ ) to achieve value near or resonate value of frequency of 2.4 GHz. The resonance frequency of 2.4 GHz occurs when  $w$  is between 2.9 mm and 3.0 mm, with a gap width of 0.02 mm. Table 2 shows the hexagon-shaped filter's aperture width of 2.92 mm resonates at 2.4 GHz, resulting in the greatest transmission coefficient ( $S_{21}$ ) values. This width size does not result in the maximum reflection coefficient value for the 1.6 GHz signal in which far more significant as the main objective to protect UAV from jamming signal. The square shape reaches resonance at 2.4 GHz with a 2.9 mm aperture width and shows the maximum reflection coefficient for the 1.6 GHz jamming signal instantly, unlike hexagon shape. The square design simplifies FSS filter development compared to the hexagon shape, which requires additional parameter adjustments, like periodic size, to align resonance frequencies.

**Table 2**  
 Simulation results for hexagon structures by varying gap widths (2.90-3.00mm)

Length	1.6 GHz		2.4 GHz	
	$S_{11}$	$S_{21}$	$S_{11}$	$S_{11}$
2.90	-1.295	-5.900	-26.965	-0.041
2.92	-1.379	-5.656	-51.226	-0.005
2.94	-1.362	-5.702	-23.311	-0.182
2.96	-1.356	-5.718	-39.019	-0.006
2.98	-1.317	-5.827	-29.152	-0.311
3.00	-1.345	-5.735	-30.347	-0.006

### 3.3 Effect of Periodic Size ( $p$ ) on the Filter Performance

Comparison on square and hexagon filters are evaluated for performance on changing period size ( $p$ ) as shown in Figures 10(a) and 10(b). Period size between 50 mm and 70 mm are tested for the square configuration, with a fixed length ( $c$ ) of 28 mm and gap width ( $w$ ) of 2.9 mm. The hexagon design is being evaluated with period changes ranging from 50 mm to 70 mm. The length of edge of each element ( $l$ ) is fixed at 24 mm and the gap width ( $w$ ) at 2.9 mm. The 40 mm period is omitted from hexagon testing due to possible collisions between shapes.



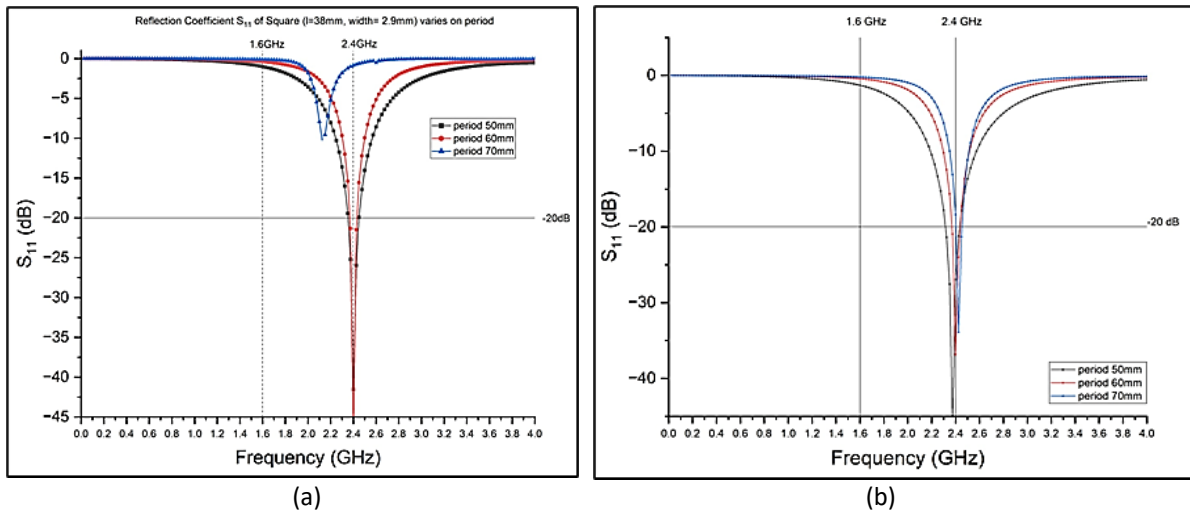


**Fig. 10.** (a) Variation of  $S_{11}$  for square (length: 38 mm, width: 2.9 mm) with different periods (50 mm, 60 mm, 70 mm) (b) Variation of  $R S_{11}$  for hexagon ( $r = 24$  mm, width = 2.9 mm) with different periods (50 mm, 60 mm, 70 mm)

To simplify, with a fixed gap of aperture of 2.9 mm and increasing period, the transient poles at  $S_{11}$  port shift to right and the bandwidth becomes narrower for hexagon shape as can be seen in Figure 11. The resonance frequency allow transmission of 2.4 GHz is now jeopardized. As the size of period increase, the strength of resonance frequency of  $S_{11}$  at 1.6 GHz decreases reaching near 0 dB. Attenuating jamming signal at 1.6 GHz is crucial as it serves the main purpose of this paper. Hence, the most optimum value generated is period at 60 mm to balance and serve objectives mainly to attenuate 1.6 GHz and allow transmission signal at 2.4 GHz.

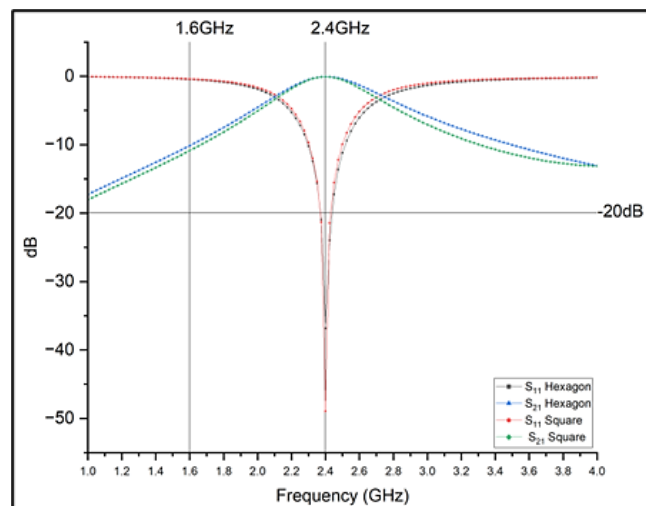


**Fig. 11.** Comparison of square and hexagon structures with a period = 60 mm

#### 4. Conclusions

In conclusion, the resonance frequency and transmission parameters in the square configuration are influenced by the array size ( $l$ ), period length ( $p$ ), and aperture width ( $w$ ). The hexagon-shaped filter shows that variations in array size affect resonance frequency, and aperture width affects resonance frequency stability at 1.6 GHz and 2.4 GHz. The period length affects signal bandwidth, as larger periods cause transient poles to shift and weaken the signal transmission of 2.4 GHz. The

resonant filter designed for the hexagon shape functions at a frequency of 2.4 GHz based on certain specifications. The advantage of square shapes are its simplicity and ease of manufacturing, consistently shows resonance behaviour across many parameters, easier to calibrate and optimise filter performance precisely. The square filter has steady resonance frequencies at 1.6 GHz and 2.4 GHz, which are important for efficient frequency selectivity. Although the hexagon shape is symmetrical, it may need complex changes to ensure stable resonance across many frequencies. The hexagon structure shows more intricate resonance behaviour, especially in terms of transient pole shifting and weakening, which could complicate the tuning process and result in less predictable filter performance. Therefore, the square shape able to provide better performance in terms of clarity, stability, and predictability for frequency-selective surface bandpass filters. Future research will entail comparing the square and hexagon shapes at identical frequencies, while also examining additional factors like angles and layers. Examining simulation findings thoroughly provides useful insights for improving resistance to jamming signals.

### Acknowledgement

This work was supported by the Ministry Higher Education of Malaysia under the Fundamental Research Grant Scheme (FRGS) Grant number (FRGS/1/2022/TK04/UNIKL/02/12).

### References

- [1] Jin, Zeyu. "Analysis of electromagnetic wave applications and development." *Highlights in Science, Engineering and Technology* 68 (2023): 172-181. <https://doi.org/10.54097/hset.v68i.12061>
- [2] Munk, Ben A. *Frequency selective surfaces: theory and design*. John Wiley & Sons, 2005.
- [3] Rabiun, Lawali, Anuar Ahmad, and Adel Gohari. "Advancements of unmanned aerial vehicle technology in the realm of applied sciences and engineering: A review." *Journal of Advanced Research in Applied Sciences and Engineering Technology* 40, no. 2 (2024): 74-95. <https://doi.org/10.37934/araset.40.2.7495>
- [4] Ramli, Nur Hidayah, Lee Yeng Seng, Liyana Zahid, and Hazry Desa. "Review on Patch Antennas for Unmanned Aerial Vehicle Application." *Journal of Advanced Research in Applied Sciences and Engineering Technology* 32, no. 3 (2023): 139-150. <https://doi.org/10.37934/araset.32.3.139150>
- [5] Norhashim, N., N. L. Mohd Kamal, Z. Sahwee, N. Lott, S. Abdul Hamid, W. N. B. Wan Jusoh, S. Ahmad, A. S. Mahmood, and A. I. Ahmad Ruzaini. "Ground Positioning System (GPS) spoofing avoidance utilizing Frequency Selective Surface (FSS) method." *Journal of Advanced Research in Dynamical and Control Systems* 12, no. 6 (2020): 1755-1760. <https://doi.org/10.5373/JARDCS/V12I2/S20201377>
- [6] Norhashim, Nurhakimah, Nadhiya Liyana Mohd Kamal, Zulhilmly Sahwee, Shahrul Ahmad Shah, Nur Afiqah Alfian, and Dinesh Sathyamoorthy. "GPS jamming impact on UAV performance in outdoor environments." *Of Manuscript* (2024): 90.
- [7] Norhashim, N., NL Mohd Kamal, Z. Sahwee, S. Ahmad Shah, and D. Sathyamoorthy. "The effects of jamming on global positioning system (GPS) accuracy for unmanned aerial vehicles (UAVs)." In *2022 International Conference on Computer and Drone Applications (IConDA)*, p. 18-22. IEEE, 2022. <https://doi.org/10.1109/ICONDA56696.2022.10000335>
- [8] Jang, Sang-Dong, Byung-Woo Kang, and Jaehwan Kim. "Frequency selective surface based passive wireless sensor for structural health monitoring." *Smart Materials and Structures* 22, no. 2 (2012): 025002. <https://doi.org/10.1088/0964-1726/22/2/025002>
- [9] Pieper, Dustin, Kristen M. Donnell, Omar Abdelkarim, and Mohamed A. ElGawady. "Embedded FSS sensing for structural health monitoring of bridge columns." In *2016 IEEE International Instrumentation and Measurement Technology Conference Proceedings*, p. 1-5. IEEE, 2016. <https://doi.org/10.1109/I2MTC.2016.7520475>
- [10] Mishrikey, Matthew, Christian Hafner, and Rüdiger Vahldieck. "Analysis and optimization of frequency selective surfaces with inhomogeneous periodic substrates." In *Optomechatronic Micro/Nano Devices and Components III*, 6717, p. 198-208. SPIE, 2007. <https://doi.org/10.1117/12.754341>
- [11] Khan, M. D. N. H., M. D. M. Alam, M. D. A. Masud, and A. A. Amin. "Importance of high order high pass and low pass filters." *World Applied Sciences Journal* 34, no. 9 (2016): 1261-1268.
- [12] Khmailia, Sameh, Hichem Taghouti, and Abdelkader Mami. "Study of a Band Stop Filter." *European Journal of Scientific Research* 95, no. 4 (2012): 582-588.

- [13] Kapoor, Ankush, Ranjan Mishra, and Pradeep Kumar. "Frequency selective surfaces as spatial filters: Fundamentals, analysis and applications." *Alexandria Engineering Journal* 61, no. 6 (2022): 4263-4293. <https://doi.org/10.1016/j.aej.2021.09.046>
- [14] Al-Joumayly, Mudar, and Nader Behdad. "A new technique for design of low-profile, second-order, bandpass frequency selective surfaces." *IEEE Transactions on Antennas And Propagation* 57, no. 2 (2009): 452-459. <https://doi.org/10.1109/TAP.2008.2011382>
- [15] Debarros, Fabien, Pierre Lemaitre-Auger, Alysson Vasconcelos Gomes de Menezes, Romain Siragusa, Tan-Phu Vuong, Guy Eymin Petot Tourtollet, and Glauco Fontgalland. "Characterization of frequency-selective surface spatial filters in a rectangular waveguide." *International Journal of Microwave and Wireless Technologies* 4, no. 1 (2012): 59-69. <https://doi.org/10.1017/S1759078711001097>
- [16] Campos, A. L. P. S., T. L. Silva, and A. Gomes Neto. "Multiband frequency selective surfaces with simple modification of a rectangular patch element." *Microwave and Optical Technology Letters* 55, no. 12 (2013): 2943-2946. <https://doi.org/10.1002/mop.27951>
- [17] Anwar, Rana Sadaf, Lingfeng Mao, and Huansheng Ning. "Frequency selective surfaces: A review." *Applied Sciences* 8, no. 9 (2018): 1689. <https://doi.org/10.3390/app8091689>
- [18] Luo, Xingfang. "Design and optimization of frequency selective surfaces (FSS)." PhD diss., Nanyang Technological University, 2006. <https://doi.org/10.32657%2F10356%2F4833>
- [19] Hussin, F. A., B. H. Ahmad, M. Z. A. A. Aziz, and M. K. Suaidi. "Design and Analysis of Frequency Selective Surface (FSS) Using Complementary Techniques on Glass." *Journal of Telecommunication, Electronic and Computer Engineering (JTEC)* 10, no. 2-8 (2018): 145-150.
- [20] Singh, Chitra, Kumud R. Jha, Satish K. Sharma, Zahoor A. Pandit Jibrán, and Ghanshyam Singh. "Design of a wideband square slot bandpass frequency-selective surface using phase range analysis." *Engineering Reports* 2, no. 1 (2020): e12085. <https://doi.org/10.1002/eng2.12085>
- [21] Ghezzi, Fabrizia, Loris Serafino, Chunlin Ji, Xigeng Miao, and Ruopeng Liu. "Deriving the Geometry of Frequency Selective Surfaces (FSS) and Metamaterials (MTM) elements from transmission lines by using surrogate meta-modeling techniques." *Progress In Electromagnetics Research* 123 (2014).
- [22] Hussein, Muaad, Yi Huang, and Jiafeng Zhou. "Frequency selective surface with miniaturized elements: A different approach."
- [23] Abadi, Seyed Mohamad Amin Momeni Hasan, and Nader Behdad. "Design of wideband, FSS-based multibeam antennas using the effective medium approach." *IEEE Transactions on Antennas and Propagation* 62, no. 11 (2014): 5557-5564. <https://doi.org/10.1109/TAP.2014.2355192>
- [24] Shim, Jongjoo, Dong Gun Kam, Jong Hwa Kwon, and Joungho Kim. "Circuit modeling and measurement of shielding effectiveness against oblique incident plane wave on apertures in multiple sides of rectangular enclosure." *IEEE Transactions on Electromagnetic Compatibility* 52, no. 3 (2010): 566-577. <https://doi.org/10.1109/TEMC.2009.2039483>
- [25] Wang, Hong Bin, and Yu Jian Cheng. "140 GHz frequency selective surface based on hexagon substrate integrated waveguide cavity using normal PCB process." *IEEE Antennas and Wireless Propagation Letters* 17, no. 3 (2018): 489-492. <https://doi.org/10.1109/LAWP.2018.2797075>
- [26] Hussein, Muaad, Zhenghua Tang, Yi Huang, and Jiafeng Zhou. "Frequency Selective Surface with High Selectivity by Adding an Inductive Layer." *Material Application in EMC* (2019): 55-61.
- [27] Hussein, Muaad Naser, Jiafeng Zhou, Yi Huang, Muayad Kod, and Abed Pour Sohrab. "Frequency selective surface structure miniaturization using interconnected array elements on orthogonal layers." *IEEE Transactions on Antennas and Propagation* 65, no. 5 (2017): 2376-2385. <https://doi.org/10.1109/TAP.2017.2684199>